Journal of Mathematical Extension
Vol. 18, No. 3, (2024) (1)1-29
URL: https://doi.org/10.30495/JME.2024.2941
ISSN: 1735-8299
Original Research Paper

An Effective Approach for Solving Nonlinear Fractional Initial Value Problems: The Fractional Legendre-Picard Iteration Method

S. Ansari
Yazd University

M. H. Akrami*
Yazd University

Abstract. The purpose of this manuscript is to present an effective numerical technique for solving nonlinear fractional differential equations. The proposed approach, known as the fractional Legendre-Picard iteration method, utilizes the shifted Legendre polynomial and the Picard iteration method. The Picard method is a recursive algorithm commonly used to solve initial value problems. However, the main challenge of this method is computing the integral of the complex and nonlinear function. In this study, we aim to approximate the function within the integral using Legendre polynomials, thereby resolving this issue. Furthermore, the fractional integrals of the shifted Legendre polynomials are easily calculated at each step. Additionally, we provide a detailed explanation of the proposed method in the form of a vector matrix, which reduces CPU time. The convergence analysis of the method is conducted, and numerical simulations are performed to demonstrate the effectiveness and accuracy of the proposed approach.

AMS Subject Classification: 34A08; 45E10.

Received: November 2023; Accepted: August 2024
*Corresponding Author

Keywords and Phrases: Fractional initial value problems, Picard iteration method, Shifted Legendre polynomials, Fractional Bratu's problem, Fractional Riccati equation.

1 Introduction

Fractional differential equations (FDEs) have become an essential tool for modeling and analyzing natural phenomena in various fields of sciences, including mathematics, physics, chemistry, and engineering [9, 16, 21, 26, 28]. Many physical processes exhibit fractional order behavior that may vary with time or space, and FDEs provide an accurate description of such behavior. These equations arise as mathematical models for physical problems, particularly those that exhibit memory effects and weak singularities [13, 27]. However, finding analytical solutions to FDEs is challenging due to the complexity of fractional derivatives and integral operators. Therefore, the development of numerical methods for solving FDEs has become an important issue. Efficient numerical techniques for approximating solutions of FDEs have been developed and studied in the last few decades.

A significant category of numerical methods for solving fractional differential equations are semi-analytical methods. Examples of such methods include: the Adomian decomposition method (ADM) and it's improvements [12, 32], variational iteration method (VIM) [19, 35], homotopy analysis method (HAM) [1, 11, 20], homotopy perturbation method (HPM) [2, 24], differential transformation method (DTM) [4, 25], and collocation methods using orthogonal polynomials such as Legendre, Chebyshev and Jacobi polynomials [3, 7, 8, 29]. These methods have been proven to be effective in solving FDEs in different scenarios, with varying degrees of accuracy and computational efficiency.

The Picard's successive method is a simple and efficient semi-analytical technique that can be used to solve a wide range of fractional differential equations [15, 23, 30]. In fact, this method is an iterative approach by generating a sequence of functions that converge to the exact solution. Each iteration involves approximating the solution with a function that depends on the previous approximation. However, this method can become complicated or unsolvable when dealing with nonlinear cases due

to the calculation of corresponding integrals. In [30], the author introduces a new method for solving fractional differential equations that combines controlled Picard's method with Simpson's rule to improve convergence and handle higher order differential equations with strong terms. In 1957, Clenshaw [10] came up with a technique that combined Chebyshev polynomials and the Picard iteration approach. This method is used to solve linear first-order ordinary differential equations. In 2010, Bai [6] modified the Chebyshev-Picard iteration method to make it even more effective for solving initial value problems (IVPs) and various types of boundary value problems (BVPs) commonly encountered in aerospace engineering. Tafakkori-Bafghi et al. in [34] introduced a method, which is based on the Picard iteration technique, to handle two-point nonlinear boundary value problems. This approach offers an effective numerical solution to such problems. Additionally, in another work [33], the authors proposed this method for solving nonlinear initial value problems. Overall, these iterative numerical methods have proved to be valuable tools in the field of (classical) numerical analysis, providing efficient solutions to various types of differential equations in different domains of application.

To the best of our knowledge, the application of orthogonal polynomials to calculate the fractional integral of nonlinear terms within the Picard's method has not been previously used to solve fractional differential equations (FDEs). In this paper, we introduce a new method called the fractional Legendre-Picard iteration method, which builds upon previous research in this area. Our proposed approach involves utilizing shifted Legendre polynomials to solve the nonlinear integral equation at each iteration of the Picard successive iteration. By doing so, we aim to provide a novel and effective numerical solution for FDEs that has not been explored before.

The purpose of this proposed method is to simplify dealing with the complexity of nonlinear terms in fractional integral in each iteration of Picard's method. It does not require specialized mathematical techniques, instead approximating the function through a recursive formula. In addition, the use of orthogonal polynomials to iteratively solve the resulting nonlinear fractional integral equation at each step of Picard's method effectively provides an exact approximation. This

approach uses orthogonal polynomials in the Picard iteration scheme to efficiently solve fractional integral equations directly, without the need for complex analytical techniques. The recursive nature and the use of orthogonal functions allow decent approximations to be computed at reasonable computational costs. As we mentioned in the article, the Legendre-Picard iteration method has advantages over the classic Picard iteration method. The advantage of our method compared to the Picard method is that in the classical Picard method, the number of terms per iteration may be significantly increased (even assuming that the integral is easily computed). However, in our method, we estimate the solution terms using Legendre polynomials and can control the number of terms. Also, the introduction of the matrix-vector form of the proposed method increases its computational speed, which can be seen in our numerical examples.

2 Preliminaries

This section presents various premises, theorems, and formulas utilized in this paper. We begin by reviewing some important concepts of fractional calculus, followed by a discussion of the properties of shifted Legendre polynomials.

Fractional calculus

Definition 2.1. [22] *The fractional integral (or the Riemann-Liouville fractional integral) with order $q > 0$, of the given function $u(t)$, $t \in (a, b)$ is defined as*

$$\begin{aligned} \mathcal{I}_a^q u(t) &= \frac{1}{\Gamma(q)} \int_a^t (t-s)^{q-1} u(s)) ds, \\ \mathcal{I}_a^0 u(t) &= u(t). \end{aligned} \tag{1}$$

Here, we need to recall the following property

$$\mathcal{I}_a^q (t-a)^k = \frac{\Gamma(k+1)}{\Gamma(q+k+1)} (t-a)^{q+k}. \tag{2}$$

The Riemann-Liouville fractional derivative of order q is represented as $\mathcal{D}^q$ and defined as follows:

$$\mathcal{D}^q u(t) = \frac{d^n}{dt^n}(\mathcal{I}_a^{n-q} u(t)),$$

where $n-1 < q \leq n, n \in \mathbb{N}$.

Definition 2.2. [22] *The Caputo derivatives with order $q > 0$ of the given function $u(t)$, $t \in (a,b)$ are defined as*

$$\begin{aligned} {}^c\mathcal{D}^q u(t) &= \frac{1}{\Gamma(n-q)} \int_a^t (t-s)^{n-q-1} u^{(n)}(s) ds, \quad n-1 \leq q \leq n, \\ &= \mathcal{I}_a^{n-q} u^{(n)}(t). \end{aligned}$$

Lemma 2.3. [22] *Let $q > 0$ and $u \in C^n[a,b]$, then*

$$\begin{aligned} &\mathcal{I}_a^{q\,c}\mathcal{D}^q u(t) = u(t) - \sum_{k=0}^{n-1} \frac{u^{(k)}(a)}{k!}(t-a)^k, \qquad t > 0, \\ &{}^c\mathcal{D}^q \mathcal{I}_a^q u(t) = u(t). \end{aligned}$$

Shifted Legendre polynomials

The Legendre polynomials, denoted as $\mathcal{L}_n(t)$ for $n = 0, 1, 2, \ldots$, form a complete set of polynomials that serve as solutions to the associated Sturm-Liouville problem [31]

$$(1-t^2)\mathcal{L}_n''(t) - 2t\mathcal{L}_n'(t) + n(n+1)\mathcal{L}_n(t) = 0, \qquad n = 0, 1, 2, \cdots .$$

The Legendre polynomials $\mathcal{L}_n(t)$ of degree n are expressed analytically as follows:

$$\mathcal{L}_n(t) = \frac{1}{\Gamma(n+1)} \sum_{k=0}^{n} \binom{n}{k} \frac{\Gamma(n+k+1)}{\Gamma(k+1)} (\frac{t-1}{2})^k.$$

where $\mathcal{L}_0(t) = 1$ and $\mathcal{L}_1(t) = t$. The set of Legendre polynomials is a complete and orthogonal system on $L^2(I) = L^2([-1,1])$ with property

$$\int_I \mathcal{L}_n(t)\mathcal{L}_m(t)\omega(t)dt = h_n \delta_{nm},$$

where $\omega(t) = 1$, $h_n = \frac{2}{2n+1}$ and δ_{nm} is the Kronecker delta function.

Now, let $\Lambda = [0, L]$. By using the change of variable $t = \frac{2}{L}t - 1$, the analytic form of the shifted Legendre polynomial is defined as:

$$\mathcal{L}_n^*(t) = \sum_{k=0}^{n} \frac{(-1)^{n-k}\Gamma(n+k+1)}{\Gamma(k+1)(n-k)!k!L^k} t^k, \tag{3}$$

where $\mathcal{L}_n^*(0) = (-1)^n$ and $\mathcal{L}_n^*(L) = 1$. Hence, the orthogonality condition is

$$\int_\Lambda \mathcal{L}_j^*(t)\mathcal{L}_k^*(t)dt = (\frac{L}{2k+1})\delta_{jk}.$$

A square integrable function $f(t)$ defined in the interval $(0, L)$ can be represented in terms of shifted Legendre polynomials as follows:

$$f(t) = \sum_{i=0}^{\infty} f_i \mathcal{L}_i^*(t),$$

where the cofficients f_i are given by

$$f_i = \frac{2i+1}{L} \int_0^L f(t)\mathcal{L}_i^*(t)dt, \quad i = 0, 1, 2, \cdots. \tag{4}$$

In practical applications, we typically consider only the first $(N+1)$ terms of the shifted Legendre polynomials. Consequently, the function $f(t)$ can be conveniently expressed in the following form:

$$f_N(t) \simeq \sum_{i=0}^{N} f_i \mathcal{L}_i^*(t) = \mathcal{B}^T \psi(t),$$

The expressions for the shifted Legendre coefficient vector $\mathcal{B}$ and the shifted Legendre vector $\psi(t)$ are as follows:

$$\mathcal{B}^T = [f_0, f_1, \cdots, f_N],$$
$$\psi(t) = [\mathcal{L}_0^*(t), \mathcal{L}_1^*(t), \cdots, \mathcal{L}_N^*(t)]^T$$

The integral in (4) can be approximated using the shifted Legendre-Gauss quadrature rule as

$$f_i \simeq (\frac{2i+1}{2}) \sum_{j=0}^{N} f(t_j)\mathcal{L}_i^*(t_j)\omega_j, \quad i = 0, 1, \cdots, N.$$

where

$$t_j = \frac{L}{2}(\tau_j + 1), \qquad j = 0, 1, \cdots, N, \tag{5}$$

and $\{\tau_j\}_{j=0}^{N}$ are the roots of $\mathcal{L}_{N+1}(t)$ and $\{\omega_j\}_{j=0}^{N}$ are corresponding weights introduced in [31] as

$$\begin{aligned}\omega_j &= \frac{2}{(1-\tau_j^2)(\mathcal{L}'_{N+1}(\tau_j))^2} \\ &= \frac{(2N+2)}{(N+1)^2\mathcal{L}_N(\tau_j)\mathcal{L}'_{N+1}(\tau_j)}, \qquad j = 0, 1, \cdots, N.\end{aligned}$$

In the continuation of the article, we need to calculate the fractional integral of shifted Legendre polynomials. Given that writing the derivative of fractional polynomials in terms of themselves is importance in the method presented in this study, we will establish this essential relationship in the following theorem.

Theorem 2.4. *Let $\mathcal{L}_n^*(t)$ be the shifted Legendre polynomials of degree n. Then we have*

$$\mathcal{I}_0^q \mathcal{L}_i^*(t) = \sum_{j=0}^{N} \varrho(i,j)\mathcal{L}_j^*(t), \qquad i = 0, 1, \cdots, N, \tag{6}$$

where

$$\varrho(i,j) = \sum_{k=0}^{i} \eta_{ijk},$$

and

$$\begin{aligned}\eta_{ijk} &= \frac{(-1)^{i-k}\Gamma(i+k+1)}{\Gamma(k+1)\Gamma(k+q+1)(i-k)!} \\ &\times \sum_{h=0}^{j} \frac{(-1)^{j-h}\Gamma(j+h+1)\Gamma(h+k+q+1)(2j+1)j!}{\Gamma(j+1)\Gamma(h+1)\Gamma(h+q+k+2)(j-h)!h!} L^q.\end{aligned} \tag{7}$$

Proof. The shifted Legendre polynomials $\mathcal{L}_n^*(t)$ of degree n are represented analytically as given in (3). Since fractional integration is a linear

operation, combining (1) and (2) leads to the following outcome:

$$\begin{aligned}\mathcal{I}_0^q\mathcal{L}_j^*(t) &= \sum_{k=0}^{j}\frac{(-1)^{j-k}\Gamma(j+k+1)}{\Gamma(k+1)(j-k)!k!L^k}\mathcal{I}^q t^k,\\ &= \sum_{k=0}^{j}\frac{(-1)^{j-k}\Gamma(j+k+1)}{\Gamma(k+1)\Gamma(q+k+1)(j-k)!k!L^k}t^{k+q}, \qquad j=0,1,\cdots N.\end{aligned} \tag{8}$$

In this step, approximate t^{k+q} by shifted Legendre series with $N+1$ terms, yields

$$t^{k+q} = \sum_{j=0}^{N} f_{kj}\mathcal{L}_j^*(t), \tag{9}$$

where f_{kj} is given from (4) with $f(t) = t^{k+q}$, that is

$$f_{kj} = (2j+1)L^{k+q} \times \sum_{h=0}^{j}\frac{(-1)^{j-h}\Gamma(j+h+1)\Gamma(h+k+q+1)}{\Gamma(h+1)\Gamma(h+q+k+2)(j-h)!h!},$$

$j = 0, 1, \cdots, N$. In virtue of (8) and (9), we get

$$\mathcal{I}_0^q\mathcal{L}_i^*(t) = \sum_{j=0}^{N}\varrho(i,j)\mathcal{L}_j^*(t), \qquad i=0,1,\cdots,N, \tag{10}$$

where

$$\varrho(i,j) = \sum_{k=0}^{i}\eta_{ijk},$$

and

$$\begin{aligned}\eta_{ijk} &= \frac{(-1)^{i-k}\Gamma(i+k+1)}{\Gamma(k+1)\Gamma(k+q+1)(i-k)!}\\ &\times \sum_{h=0}^{j}\frac{(-1)^{j-h}\Gamma(j+h+1)\Gamma(h+k+q+1)(2j+1)j!}{\Gamma(j+1)\Gamma(h+1)\Gamma(h+q+k+2)(j-h)!h!}L^q.\end{aligned}$$

Therefore, the desired result is obtained from Equation (7). □

Remark 2.5. *Based on Theorem 2.4, in the vector form we have [8]:*

$$\mathcal{I}_0^q\mathcal{L}_i^*(t) \simeq [\varrho(i,0), \varrho(i,1), \cdots, \varrho(i,N)]\psi(t), \qquad i=0,1,\cdots,N.$$

3 Fractional Legendre-Picard's iteration method

In this section, our proposed method named as the fractional Legendre-Picard's iteration method (FLPIM) provides an iterative algorithm for solving fractional ordinary differential equations (FODEs) of the form

$$ {}^{c}\mathcal{D}^{q}u(t) = f(t,u(t)), \qquad 0<t<L, \qquad n-1\leq q\leq n, \quad n\in\mathbb{N}, \tag{11} $$

$$ u^{(l)}(0) = u_0^{(l)}, \qquad l=0,1,\cdots n-1, \tag{12} $$

where ${}^{c}\mathcal{D}^{q}u(t)$ is the Caputo fractional differential operator of order $q>0$. By applying fractional integration to both sides of equation (11) and utilizing Lemma 2.3, we can equivalently express the fractional problem (11) with initial conditions (12) as a fractional integral equation equation:

$$ u(t) = \sum_{l=0}^{n-1}\frac{t^l u_0^{(l)}}{l!} + \frac{1}{\Gamma(q)}\int_0^t (t-s)^{q-1} f(s,u(s))ds. \tag{13} $$

In accordance with (13), the sequence of Picard's iterations is generated as follows:

$$ u^i(t) = \sum_{l=0}^{n-1}\frac{t^l u_0^{(l)}}{l!} + \frac{1}{\Gamma(q)}\int_0^t (t-s)^{q-1} f(s,u^{i-1}(s))ds, \tag{14} $$

where $u^0(t)$ represents an appropriate initial function that fulfils the given initial condition. During the first step of the FLPIM, we approximate the function $f(s,u^{i-1}(s))$ on the right side of equation (14) using the set $\{\mathcal{L}_n^*(s)\}_{n=0}^N$.Therefore,

$$ f(s,u^{i-1}(s)) \simeq \sum_{j=0}^{N}\tilde{f}_j^{i-1}\mathcal{L}_j^*(s), \tag{15} $$

where the coefficients $\{\tilde{f}_j^{i-1}\}_{j=0}^N$ can be obtained as

$$ \tilde{f}_j^{i-1} = \Big(\frac{2j+1}{2}\Big)\sum_{k=0}^{N} f(t_k,u^{i-1}(t_k))\mathcal{L}_j^*(t_k)\omega_k, \qquad j=0,1,\ldots,N. \tag{16} $$

Substituting (15) in (14),we have

$$u^i(t) = \sum_{l=0}^{n-1} \frac{t^l u_0^{(l)}}{l!} + \mathcal{I}^q(f(t,u(t))) \simeq \sum_{l=0}^{n-1} \frac{t^l u_0^{(l)}}{l!} + \mathcal{I}^q\Big(\sum_{j=0}^{N} \tilde{f}_j^{i-1} \mathcal{L}_j^*(t)\Big)$$
$$= \sum_{l=0}^{n-1} \frac{t^l u_0^{(l)}}{l!} + \sum_{j=0}^{N} \tilde{f}_j^{i-1} \mathcal{I}^q\Big(\mathcal{L}_j^*(t)\Big).$$

According to (9) and (10), we have

$$u^i(t) = \sum_{l=0}^{n-1} \frac{u_0^{(l)}}{l!} \sum_{j=0}^{N} C_{lj} \mathcal{L}_j^*(t) + \sum_{k=0}^{N} \tilde{f}_k^{i-1} \sum_{j=0}^{N} \varrho(k,j) \mathcal{L}_j^*(t)$$
$$= \sum_{j=0}^{N} \mathcal{L}_j^*(t) \sum_{l=0}^{n-1} \frac{u_0^{(l)}}{l!} C_{lj} + \sum_{k=0}^{N} \tilde{f}_k^{i-1} \sum_{j=0}^{N} \varrho(k,j) \mathcal{L}_j^*(t)$$
$$= \sum_{j=0}^{N} \mathcal{L}_j^*(t) \Big(\sum_{l=0}^{n-1} \frac{u_0^{(l)}}{l!} C_{lj} + \sum_{k=0}^{N} \tilde{f}_k^{i-1} \varrho(k,j) \Big). \tag{17}$$

where

$$C_{lj} = (2j+1) L^l \times \sum_{f=0}^{j} \frac{(-1)^{j-f} \Gamma(j+f+1) \Gamma(f+l+1)}{\Gamma(f+1) \Gamma(f+l+2) (j-f)! f!}.$$

Now, we consider the approximation of $u^i(t)$ as follows

$$u^i(t) \simeq \sum_{j=0}^{N} a_j^i \mathcal{L}_j^*(t). \tag{18}$$

Using (17) and (18), we obtain

$$a_0^i \mathcal{L}_0^*(t) + a_1^i \mathcal{L}_1^*(t) + \cdots + a_N^i \mathcal{L}_N^*(t) \simeq \mathcal{L}_0^*(t) \Big(\sum_{l=0}^{n-1} \frac{u_0^{(l)}}{l!} C_{l0} + \sum_{k=0}^{N} \tilde{f}_k^{i-1} \varrho(k,0) \Big)$$
$$+ \cdots + \mathcal{L}_N^*(t) \Big(\sum_{l=0}^{n-1} \frac{u_0^{(l)}}{l!} C_{lN} + \sum_{k=0}^{N} \tilde{f}_k^{i-1} \varrho(k,N) \Big). \tag{19}$$

The coefficients $\{a_j^i\}_{j=0}^N$ are determined by equating the coefficients of the shifted Legendre polynomials from the first to the N^{th} order on both sides of equation (19), which ultimately results in the value

$$a_j^i = \sum_{l=0}^{n-1} \frac{u_0^{(l)}}{l!} C_{lj} + \sum_{k=0}^{N} \tilde{f}_k^{i-1} \varrho(k,j), \qquad j = 0, 1, \cdots N. \tag{20}$$

Therefore, by determining the values of a_j^i, we can make an approximation of $u^i(t)$. The updated coefficients allow us to refine the approximation of the integrand in equation (14) for each subsequent iteration. This iterative process will continue until the desired level of accuracy is achieved. The FLPIM algorithm will keep iterating until the stopping criterion is met, which is defined as:

$$\|u^i(t) - u^{i-1}(t)\| = \max_{t\in[0,L]} |u^i(t) - u^{i-1}(t)| < \epsilon,$$

where ϵ is a predefined tolerance.

We summarize the FLPI method in the following algorithm.

Input:

- Fractional order q
- Number of initial conditions n
- Number of Legendre polynomials N
- Domain length L
- Tolerance ϵ
- Initial function $u_0(t)$ that satisfies the given initial conditions

Output: Approximate solution $u(t)$ to the fractional ODE
Algorithm:

1. Initialize $u^0(t) \leftarrow u_0(t)$
2. Calculate the coefficients C_{lj} using the Legendre weights and Legendre polynomials.

3. Perform Picard iterations until the stopping criterion is met:
   - For each $j = 0, 1, \ldots, N$ do:
     - Calculate the coefficients $\tilde{f}_j^{i-1}$ using the formula (16)
     - Calculate the coefficients a_j^i using the formula (20)
     - Update the approximation $u^i(t)$ using the formula:

$$u^i(t) \leftarrow \sum_{j=0}^{N} a_j^i \cdot \mathcal{L}_j^*(t)$$

   - Check if the stopping criterion is met:

$$\max_{t\in[0,L]} |u^i(t) - u^{i-1}(t)| < \epsilon$$

   - If the criterion is met, stop the iterations.
   - Otherwise, update the previous approximation for the next iteration: $u^{i-1} \leftarrow u^i$
4. Return the final approximation $u(t)$.

Vector-Matrix form of the FLPIM

To improve the speed and efficiency of the FLPIM, we introduce a compact vector-matrix representation. In order to approximate the solution $u^i(t)$, we determine the coefficients $\{a_j^i\}_{j=0}^N$ of the shifted Legendre polynomials using the expression (18). For ease of computation, we represent the coefficients of the approximate solution $u^i(t)$ in vector format as:

$$\boldsymbol{a}^i = [a_0, a_1, \cdots, a_N]^T,$$

Additionally, we consider the solution $u^i(t)$ evaluated at the shifted Legendre-Gauss nodes (5) in a vector form.

$$\boldsymbol{u}^i = [u^i(t_0), u^i(t_1), \cdots, u^i(t_N)]^T. \tag{21}$$

substituting (18) in (21), the vector u^i can be obtained as

$$\boldsymbol{u}^i = \mathbb{L}_{\boldsymbol{u}} \boldsymbol{a}^i.$$

where

$$\mathbb{L}_{\boldsymbol{u}} = \begin{pmatrix} \mathcal{L}_0^*(t_0) & \mathcal{L}_1^*(t_0) & \cdots & \mathcal{L}_N^*(t_0) \\ \mathcal{L}_0^*(t_1) & \mathcal{L}_1^*(t_1) & \cdot & \mathcal{L}_N^*(t_1) \\ \vdots & \vdots & \ddots & \cdots \\ \mathcal{L}_0^*(t_N) & \mathcal{L}_1^*(t_N) & \cdots & \mathcal{L}_N^*(t_N) \end{pmatrix},$$

is a constant matrix. Now, by using (20), the vector a^i can be calculated in the new form

$$\boldsymbol{a}^i = \begin{pmatrix} a_0^i \\ a_1^i \\ \vdots \\ a_N^i \end{pmatrix} = \begin{pmatrix} \sum_{l=0}^{n-1} \frac{u_0^{(l)}}{l!} C_{l0} + \sum_{k=0}^{N} \tilde{f}_k^{i-1} \varrho(k,0) \\ \sum_{l=0}^{n-1} \frac{u_0^{(l)}}{l!} C_{l1} + \sum_{k=0}^{N} \tilde{f}_k^{i-1} \varrho(k,1) \\ \vdots \\ \sum_{l=0}^{n-1} \frac{u_0^{(l)}}{l!} C_{lN} + \sum_{k=0}^{N} \tilde{f}_k^{i-1} \varrho(k,N) \end{pmatrix} \tag{22}$$

$$= \boldsymbol{u}_a + \begin{pmatrix} \tilde{f}_0^{i-1}\varrho(0,0) + \tilde{f}_1^{i-1}\varrho(1,0) + \cdots + \tilde{f}_N^{i-1}\varrho(N,0) \\ \tilde{f}_0^{i-1}\varrho(0,1) + \tilde{f}_1^{i-1}\varrho(1,1) + \cdots + \tilde{f}_N^{i-1}\varrho(N,1) \\ \vdots \\ \tilde{f}_0^{i-1}\varrho(0,N) + \tilde{f}_1^{i-1}\varrho(1,N) + \cdots + \tilde{f}_N^{i-1}\varrho(N,N) \end{pmatrix}$$

$$= \boldsymbol{u}_a + \begin{pmatrix} \varrho(0,0) & \varrho(1,0) & \cdots & \varrho(N,0) \\ \varrho(0,1) & \varrho(1,1) & \cdots & \varrho(N,1) \\ \vdots & & & \\ \varrho(0,N) & \varrho(1,N) & \cdots & \varrho(N,N) \end{pmatrix} \begin{pmatrix} \tilde{f}_0^{i-1} \\ \tilde{f}_1^{i-1} \\ \vdots \\ \tilde{f}_N^{i-1} \end{pmatrix} = \boldsymbol{u}_a + \boldsymbol{M}\boldsymbol{f}^{\boldsymbol{i-1}},$$

where

$$\boldsymbol{u}_a = \left(\sum_{l=0}^{n-1} \frac{u_0^l}{l!} C_{l0}, \quad \sum_{l=0}^{n-1} \frac{u_0^l}{l!} C_{l1}, \quad \cdots, \quad \sum_{l=0}^{n-1} \frac{u_0^l}{l!} C_{lN} \right)^T,$$

$$\boldsymbol{f}^{\boldsymbol{i-1}} = \left(\tilde{f}_0^{i-1}, \quad \tilde{f}_1^{i-1}, \quad \cdots, \quad \tilde{f}_N^{i-1} \right)^T, \tag{23}$$

In this context, $\boldsymbol{u}_a$ represents a fixed vector, and $\boldsymbol{M}$ is a constant matrix. Now, applying (16) in (23), we obtain the following:

$$\begin{aligned}
\boldsymbol{f^{i-1}} &= \begin{pmatrix} \tilde{f}_0^{i-1} \\ \tilde{f}_1^{i-1} \\ \vdots \\ \tilde{f}_N^{i-1} \end{pmatrix} \\
&= \begin{pmatrix} \frac{1}{2}\Big(f(t_0,u^{i-1}(t_0))\mathcal{L}_0^*(t_0)\omega_0+\cdots+f(t_N,u^{i-1}(t_N))\mathcal{L}_0^*(t_N)\omega_N\Big) \\ \frac{3}{2}\Big(f(t_0,u^{i-1}(t_0))\mathcal{L}_1^*(t_0)\omega_0+\cdots+f(t_N,u^{i-1}(t_N))\mathcal{L}_1^*(t_N)\omega_N\Big) \\ \vdots \\ \frac{2N+1}{2}\Big(f(t_0,u^{i-1}(t_0))\mathcal{L}_N^*(t_0)\omega_0+\cdots+f(t_N,u^{i-1}(t_N))\mathcal{L}_N^*(t_N)\omega_N\Big) \end{pmatrix} \\
&= \boldsymbol{E}\mathbb{L}_u^T\boldsymbol{W}\boldsymbol{F^{i-1}} \qquad (24)
\end{aligned}$$

where

$$\boldsymbol{W} = diag\left(\omega_0,\omega_1,\cdots,\omega_N\right)_{N+1},$$

$$\boldsymbol{E} = diag\left(\tfrac{1}{2},\tfrac{3}{2},\cdots,\tfrac{2N+1}{2}\right)_{N+1},$$

$$\boldsymbol{F^{i-1}} = \left(f(t_0,u^{i-1}(t_0)),f(t_1,u^{i-1}(t_1)),\cdots,f(t_N,u^{i-1}(t_N))\right)^T,$$

Thus, from (22) and (24), one can get

$$\boldsymbol{a}^i = \boldsymbol{u}_a + \boldsymbol{M}\boldsymbol{f}^{i-1} = \boldsymbol{u}_a + \boldsymbol{M}\boldsymbol{E}\mathbb{L}_u^T\boldsymbol{W}\boldsymbol{F^{i-1}} = \boldsymbol{u}_a + \mathbb{L}_a^T\boldsymbol{F^{i-1}},$$

where $\mathbb{L}_a = \boldsymbol{M}\boldsymbol{E}\mathbb{L}_u^T\boldsymbol{W}$ is a constant matrix. In the FLPI method $\boldsymbol{a}^i$ will be updated until until the desired level of accuracy is achieved. Here, we consider the following stopping condition for V-MF (vector-matrix form)

$$\|\boldsymbol{u}^i - \boldsymbol{u}^{i-1}\| = \max_{0\le j\le N}|u^i(t_j) - u^{i-1}(t_j)| < \epsilon,$$

where ϵ is a given tolerance.

Because the coefficient matrices $\mathbb{L}_u^T$ and $\mathbb{L}_a$ remain unchanged throughout all iterations, we can compute them once before the loop and reuse them thereafter. As a result, the V-MF of the FLPI method is computationally more efficient compared to the standard iterative form (IF).

4 Convergence Analysis of the FLPI method

When introducing a numerical method for solving differential equations, a crucial aspect of investigation revolves around the method's convergence characteristics and determining its convergence domain. In the case of the FLPI method, a modification of the Chebyschev-Picard and Jacobi-Picard methods [6, 33], its convergence domain differs from the classical Picard iteration method [34]. The observed difference can be attributed to the accumulation of round-off error and approximation error arising from the truncated shifted Legendre series of order N employed during the iterations. In this context, drawing upon the concepts discussed in [6, 33], we demonstrate that the convergence of the FLPI method is not guaranteed globally. However, we can establish a specific condition that ensures its convergence. For achieve this objective, let us consider fractional ordinary differential equations (11) with initial condition (12). We present the convergency condition of the FLPIM in the following theorem.

Theorem 4.1. *Suppose in fractional ordinary differential equations* (11) *with initial condition* (12)*, the function f satisfied in the Lipschitz condition with respect to the second variable, i.e.*

$$|f(t,u) - f(t,v)| \leq K|u - v|.$$

The FLPI method is convergence if and only if $\|\mathbb{L}_u\mathbb{L}_a\| < \frac{1}{K}$.

Proof. We work with V-MF of the our method. Therefore, from (3) we have

$$\begin{aligned}
\boldsymbol{u}^i - \boldsymbol{u}^{i-1} &= \mathbb{L}_u\boldsymbol{a}^i - \mathbb{L}_u\boldsymbol{a}^{i-1} = \mathbb{L}_u\Big(\boldsymbol{a}^i - \boldsymbol{a}^{i-1}\Big) \\
&= \mathbb{L}_u\Big(\boldsymbol{u}_a + \mathbb{L}_a\boldsymbol{F}^{i-1} - \boldsymbol{u}_a - \mathbb{L}_a\boldsymbol{F}^{i-2}\Big) \\
&= \mathbb{L}_u\mathbb{L}_a\Big(\boldsymbol{F}^{i-1} - \boldsymbol{F}^{i-2}\Big) \\
\|\boldsymbol{u}^i - \boldsymbol{u}^{i-1}\| &= \|\mathbb{L}_u\mathbb{L}_a\Big(\boldsymbol{F}^{i-1} - \boldsymbol{F}^{i-2}\Big)\| \\
&\leq \|\mathbb{L}_u\mathbb{L}_a\|\|\boldsymbol{F}^{i-1} - \boldsymbol{F}^{i-2}\|
\end{aligned}$$

$$\begin{aligned}
&\leq \|\mathbb{L}_u\mathbb{L}_a\| \max_{0\leq j\leq N} |f(t_j, u^{i-1}(t_j)) - f(t_j, u^{i-2}(t_j))| \\
&\leq \|\mathbb{L}_u\mathbb{L}_a\| \max_{0\leq j\leq N} K|u^{i-1}(t_j) - u^{i-2}(t_j)| \\
&= K\|\mathbb{L}_u\mathbb{L}_a\| \max_{0\leq j\leq N} K|u^{i-1} - u^{i-2}| \\
&= K\|\mathbb{L}_u\mathbb{L}_a\|\|u^{i-1} - u^{i-2}\|.
\end{aligned}$$

Then

$$\begin{aligned}
\|\boldsymbol{u}^i - \boldsymbol{u}^{i-1}\| &\leq K\|\mathbb{L}_u\mathbb{L}_a\|\|u^{i-1} - u^{i-2}\| \\
&\leq (K\|\mathbb{L}_u\mathbb{L}_a\|)^2\|u^{i-2} - u^{i-3}\| \\
&\leq (K\|\mathbb{L}_u\mathbb{L}_a\|)^3\|u^{i-3} - u^{i-4}\| \\
&\vdots \\
&\leq (K\|\mathbb{L}_u\mathbb{L}_a\|)^{i-1}\|u^1 - u^0\|.
\end{aligned}$$

Accordingly, we will have

$$\|\boldsymbol{u}^i - \boldsymbol{u}^{i-1}\| \leq (K\|\mathbb{L}_u\mathbb{L}_a\|)^{i-1}\|u^1 - u^0\|.$$

Hence, it is clear that if, $\|\mathbb{L}_u\mathbb{L}_a\| < \frac{1}{K}$ we will obtain

$$\lim_{i\to\infty} \|u^i - u^{i-1}\| = 0,$$

which completes the proof. □

5 Numerical Examples

In this section, we demonstrate the effectiveness and precision of the FLPI method through various examples. Our comparison of results obtained from other methods highlights the high accuracy and efficiency of the FLPI method.

Example 5.1. The following initial value problem is considered:[30],

$$\begin{aligned}
{}^c\mathcal{D}^q u(t) &= t^8\exp(t) + \frac{\Gamma(5)}{\Gamma(5-q)}t^{4-q} - \exp(t)u^2(t), \qquad 2 \leq q \leq 3, \\
u(0) &= u'(0) = u''(0) = 0, \qquad\qquad 0 \leq t \leq 1,
\end{aligned}$$

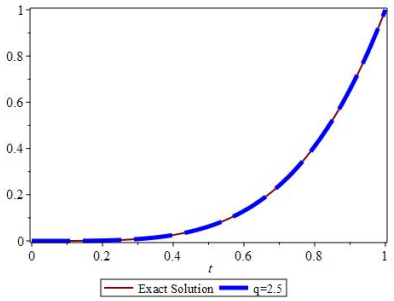

(a) the comparison of approximate solutions for $q = 2.5$ with exact solution.

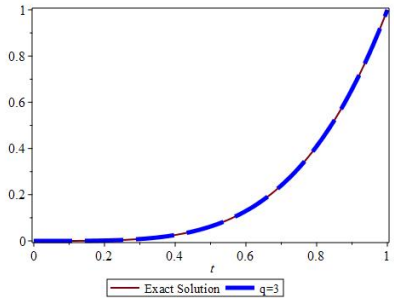

(b) the comparison of approximate solutions for $q = 3$ with exact solution.

Figure 1: The exact and approximate solutions for $q = 2.5$ and $q = 3$ in Example 5.1.

and has the exact solution $u(t) = t^4$. Figure 1 illustrates a comparison between the exact and approximate solutions for various q orders.

The exact and approximate solutions exhibit a close match, indicating that the approximate method effectively addresses the given problem with significant reductions in computational time and resources compared to the exact method. The approximate solution follows similar trends and shapes as the exact one.

To demonstrate our new approach, we approximated the absolute errors of the scheme at different q orders and combined the results with those from [30], using the controlled Picard's method with Simpson rule. Figures 2(a) and 2(b) present the visualized results.

Comparing the absolute errors shown in Figures 2(a) and 2(b), it's evident that our new method has reduced the error by 10^3 times compared to the controlled Picard's method with Simpson rule [30]. Thus, the our new FLPI method proves highly accurate for solving equations when compared to the controlled Picard's method with Simpson rule. For N=30, Table 1 displays the maximum absolute error and CPU time obtained by the proposed method.

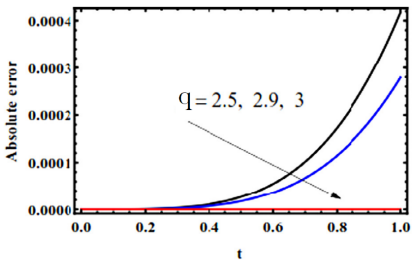

(a) Absolute error of solution by the method presented in [30].

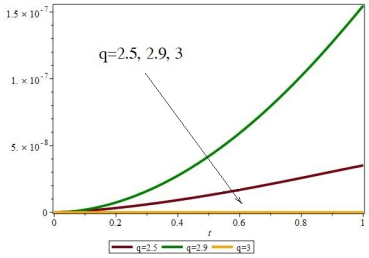

(b) Absolute error of solution by the FLPI method of Example 5.1.

Figure 2: Comparison of solution by our FLPI method and controlled Picard's method with Simpson rule of [30].

Table 1: The maximum absolute error and iteration numbers (IN) achieved by the FLPI method, employing a stopping criterion of $\epsilon = 10^{-30}$ for Example 5.1.

q	L_∞	IN	CPU time, s
2.5	$3.513600e-08$	10	1.156
2.9	$1.547222e-07$	9	1.297
3	$2.057261e-36$	8	0.89

The primary focus of many scientists has always been on modeling and solving real-world problems. One such problem is Bratu's problem, which originated as a simplification of the solid fuel ignition model in thermal combustion theory. Recently, researchers have extended Bratu's problem to include fractional derivatives in some papers, such as the one by Ghomanjani et al [18]. In this study, we tackle this extended problem using the FLPI method, as demonstrated in the following example.

Example 5.2. The fractional Bratu's initial value problem (FBIVP) is considered [18]

$$\begin{aligned} {}^{c}\mathcal{D}^{q}u(t) &= 2\exp(u(t)), & 1 < q \leq 2, \\ u(0) = u'(0) &= 0, & 0 < t < 1, \end{aligned}$$

The exact solution by $q = 2$ is $u(t) = -2\ln(\cos(t))$. In Figure 3, we

illustrate the exact solution and approximate solutions of FBIVP for $q = 2$.

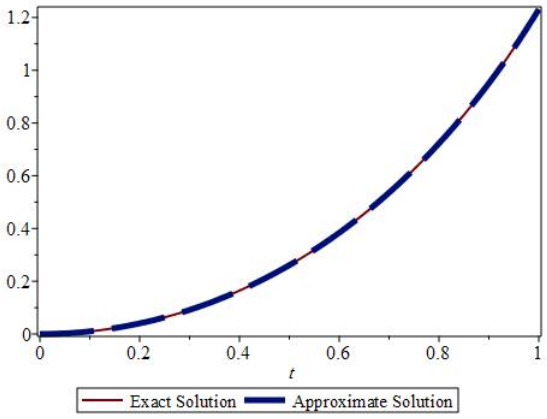

Figure 3: The exact and approximate solutions for $q = 2$ in Example 5.2.

The exact and approximate solutions exhibit a remarkable agreement, signifying that the approximate method provides a robust solution to the given problem while significantly reducing the computational time and resource requirements compared to the exact method. The approximate solution closely matches with the general trends and shapes observed in the exact solution.

To efficiently demonstrate our novel approach (FLPI method), we computed the maximum absolute errors of the scheme at $q = 2$ and $q = 1.9$. These results were then combined with the findings from [18] and [17], alongside the maximum absolute errors obtained from the Bezier curve method (BCM) [18], compact finite difference scheme (CFDS) [17], and the proposed reproducing kernel method (RKM) [5]. The visualized outcomes are presented in Table 2.

Example 5.3. Consider the following fractional initial value problem

$$
\begin{aligned}
{}^{c}\mathcal{D}^{q}u(t) &= \frac{\Gamma(9)}{\Gamma(9-q)}t^{8-q} + t^{8} + \frac{9}{4}t^{q} + \frac{9}{4}\Gamma(q+1) - u(t), \qquad 0 < q < 1,\\
u(0) &= 0, \qquad\qquad t \in [0, L],
\end{aligned}
$$

Table 2: The maximum absolute error of solution by our method with RKM, CFDS and BCM for $q = 2, 1.9$, of Example 5.2.

q	proposed method	error of RKM [5]	error of CFDS [17]	error of BCM [18]
2	$1.42e-19$	$2.12e-4$	$8.32e-5$	$3.47e-3$
1.9	$2.01e-01$	1.43	1.46	1.23

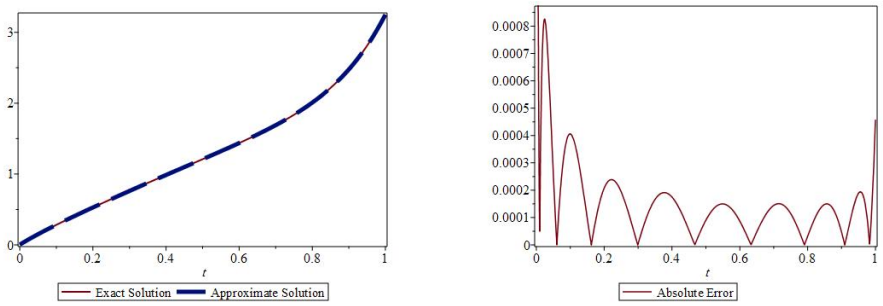

(a) Comparison of the exact and approximate solutions of Example 5.3.

(b) Absolute error of solution by proposed method of Example 5.3.

Figure 4: Solution of proposed method for $q = 0.9$.

whose exact solution is given by $u(t) = \frac{9}{4}t^q + t^8$.
The graph of the exact and approximate solutions are illustrated in Figure 4(a) and absolute error of solution by proposed FLPI method is presented in Figure 4(b). We observe a close alignment between the exact and approximation solutions, as demonstrated in Table 3, which presents the maximum absolute error and CPU time for the iterative form (IF) and V-MF of the FLPIM with a stopping criterion of $\epsilon = 10^{-30}$. Observing across all modes, it is evident that the V-MF exhibits notably faster performance. Table 4 presents the maximum error of the FLPIM for various values of N, along with the stopping criterion $\epsilon = 10^{-30}$ and the corresponding IN. As we increase the value of N, we observe a notable exponential decrease in errors.

Example 5.4. Consider the following fractional Riccati differential equation (FRDE) [14],

$$\begin{aligned} {}^{c}\mathcal{D}^{q}u(t) &= 1 + u^2(t), & 0 < q \leq 1, \\ u(0) &= 0, & t \in [0, 1], \end{aligned}$$

Table 3: A comparative analysis of CPU time (in seconds) between the IF and V-MF of the FLPIM with a stopping criterion of $\epsilon = 10^{-30}$ for Example 5.3.

q	N	4	8	16	32
0.5	IF	6.281	13.156	39.719	416.032
	V-MF	1.312	1.344	1.266	2.125
0.9	IF	4.063	7.813	24.641	185.016
	V-MF	1.063	1.141	1.125	1.547
1	IF	2.625	4.328	13.172	109.406
	V-MF	1.469	1.031	1.344	1.687

Table 4: The maximum errors obtained by the FLPIM for different values of N and a stopping criterion of $\epsilon = 10^{-30}$, along with the corresponding IN for Example 5.3.

N / q	32		16		8		4	
	Error	IN	Error	IN	Error	IN	Error	IN
0.9	$4.210158e-04$	32	$1.394541e-03$	32	$4.429987e-03$	36	$4.593985e-02$	40
1	$8.482475e-33$	29	$8.482163e-33$	29	$2.730550e-32$	32	$3.314523e-02$	38

The exact solution for $q = 1$ is given by $u(t) = \tan(t)$.
Figure 5(a) presents the exact and approximate solutions, while figure 5(b) shows the absolute error of the solution obtained by the FLPI method. Figure 6 illustrates the approximate and exact solutions at different q orders and $N = 20$ for the FRDE. To demonstrate the effectiveness of our new approach, we first calculated the maximum absolute errors of the scheme at $q = 1$. Next, we integrated these results with the findings from [14], which also included the maximum absolute errors obtained by a decomposition algorithm using spectral methods [14]. The combined results are presented in Table 5 for visualization.

Example 5.5. Consider the nonlinear fractional differential equation [25],

$$\begin{aligned} {}^{c}\mathcal{D}^{q}u(t) &= \sin(t)\cos^{2}(t) - 2u(t) + u^{3}(t), \qquad 1 < q \leq 2, \\ u(0) &= 0, \qquad u'(0) = 1, \qquad 0 \leq t \leq 1, \end{aligned}$$

In the case of $q = 2$, the exact solution is given by $u(t) = \sin(t)$.

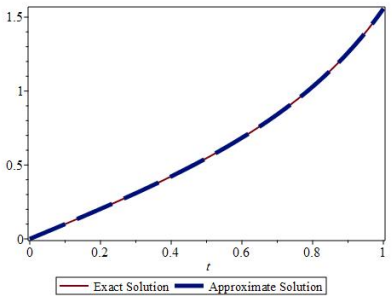

(a) The approximate and exact solutions of Example 5.4.

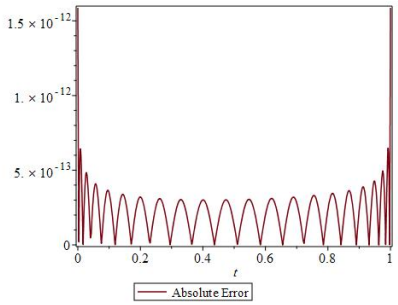

(b) Absolute error of solution by proposed method of Example 5.4.

Figure 5: Solution of proposed method for $q = 1$.

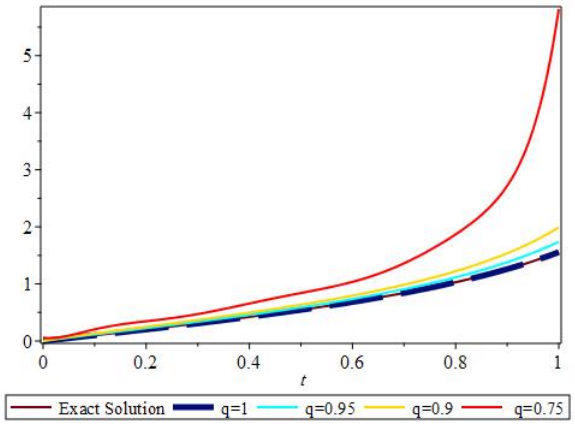

Figure 6: The approximate and exact solutions at different q orders and $N = 20$ for Example 5.4.

Table 5: Absolute errors of $u(t)$ using the proposed method versus the spectral methods [14] with $q = 1$ for Example 5.4.

N	proposed method	spectral methods [14]
4	$4.0219e-03$	$6.9682e-3$
8	$1.9667e-05$	$2.0857e-5$
12	$8.8374e-08$	$7.3355e-8$

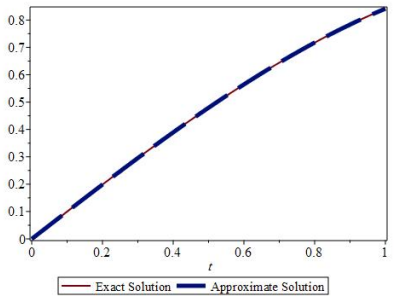

(a) The exact and approximate solutions of Example 5.5 for $q = 2$ and $N = 10$.

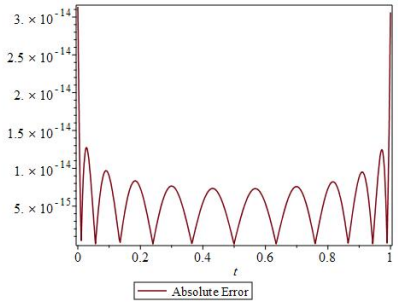

(b) Absolute error of solution by the FLPI method in Example 5.5 for $q = 2$ and $N = 10$.

Figure 7: The solution and absolute error corresponding to Example 5.5.

Table 6: Maximum of the absolute error of the FLPIM with stopping criterion $\epsilon = 10^{-30}$ Example 5.5 for $q = 2$.

N	4	8	12	16	32
L_∞	$2.933034e-05$	$5.008585e-11$	$1.361912e-17$	$1.061507e-24$	$4.033158e-34$
IN	5	16	14	14	14

Figure 7(a) shows the graph of the exact solution and approximate solutions, and figure 7(b) displays the absolute error of the solution computed by the FLPI method. The excellent agreement between the exact and approximate solutions signifies that the proposed approximate method offers a commendable solution to the problem, all the while significantly reducing computational time and resource requirements in comparison to the exact method. Moreover, the approximate solution closely adheres to the trends and shapes observed in the exact solution. Table 6 presents a comparison of the maximum absolute error for various values of N alongside its corresponding IN. The results highlight that increasing the value of N leads to improved accuracy in the proposed method. To showcase the efficiency of the FLPIM, Table 7 provides a comparative analysis of the maximum absolute error with other methods mentioned in the study. This comparison underscores the competitiveness and efficacy of the FLPIM in delivering accurate results.

Table 7: Comparison of maximum errors between the FLPIM ($N = 5, 10, \epsilon = 10^{-30}$) and several methods for Example 5.5 for $q = 2$.

N	proposed method	modified HAM [25]	HAM [25]	FDE12
5	$7.627515e-07$	$1.2e-5$	$5e-3$	$6.076221e-4$
10	$3.134866e-14$	$1.5e-9$	$2.5e-6$	$6.076221e-4$

By increasing the value of N, we observe a significant exponential decrease in errors, highlighting the enhanced accuracy of our approach. To effectively demonstrate the merits of our new method, we first computed the maximum absolute errors of the scheme at $q = 2$. Subsequently, we integrated these results with the findings of [25], which included the maximum absolute errors obtained using the homotopy analysis method (HAM) [25] and its modified algorithm. The combined outcomes are presented in Table 7 for comprehensive visualization and analysis.

6 Conclusion

In this work, we introduced the FLPIM as a powerful numerical tool for solving nonlinear fractional differential equations. By combining the Picard iteration method, orthogonal shifted Legendre polynomials, and the shifted Legendre-Gauss quadrature formula, we developed the FLPIM, which stands out for its simplicity and efficiency.

The FLPIM eliminates the need for derivative or integral computations, making it easy to implement without Taylor series approximations, Adomian decomposition, or solving systems of algebraic equations. Instead, the integration of shifted Legendre polynomials is analytically computed using an iterative formula, as stated in Theorem 2.4. We further introduced a V-MF variant of the FLPIM to enhance its computational speed.

To assess the method's performance, we applied it to well-known and practical problems in fractional differential equations, such as the fractional Riccati and fractional Bratu's problems. The accuracy of the FLPIM's results was verified by comparing them with solutions obtained from various established numerical methods in the literature, showcasing the method's reliability and effectiveness.

We also conducted a convergence analysis of the proposed method and determined the conditions for its convergence.

In conclusion, the FLPIM provides a robust and efficient approach for solving nonlinear fractional differential equations, delivering accurate results while offering notable computational advantages. This work contributes to the field of fractional calculus and provides valuable insights for future advancements and applications in this domain.

References

[1] S. Abbasbandy, M. Hashemi, and I. Hashim. On convergence of homotopy analysis method and its application to fractional integro-differential equations. *Quaestiones Mathematicae*, 36(1) (2013), 93–105.

[2] O. Abdulaziz, I. Hashim, and S. Momani. Application of homotopy-perturbation method to fractional ivps. *Journal of Computational and Applied Mathematics*, 216(2) (2008), 574–584.

[3] M. H. Akrami, M. H. Atabakzadeh, and G.H. Erjaee. The operational matrix of fractional integration for shifted legendre polynomials. *Iranian journal of science and technology. Transaction A, Science*, 37(A4) (2013), 439–444.

[4] A. Arikoglu and I. Ozkol. Solution of fractional differential equations by using differential transform method. *Chaos, Solitons & Fractals*, 34(5) (2007), 1473–1481.

[5] E. Babolian, S. Javadi, and E. Moradi. RKM for solving Bratu-type differential equations of fractional order. *Mathematical Methods in the Applied Sciences*, 39(6) (2016), 1548–1557.

[6] X. Bai. *Modified Chebyshev-Picard Iteration Methods for Solution of Initial Value and Boundary Value Problems*. PhD thesis, Texas A&M University, (2010).

[7] A. H. Bhrawy. A jacobi spectral collocation method for solving multi-dimensional nonlinear fractional sub-diffusion equations. *Numerical Algorithms*, 73 (2016), 91–113.

[8] A. H. Bhrawy and A. Alofi. The operational matrix of fractional integration for shifted chebyshev polynomials. *Applied Mathematics Letters*, 26(1) (2013), 25–31.

[9] A. C. Cevikel and E. Aksoy. Soliton solutions of nonlinear fractional differential equations with their applications in mathematical physics. *Revista mexicana de física*, 67(3), (2021), 422–428.

[10] C. Clenshaw. The numerical solution of linear differential equations in chebyshev series. In *Mathematical Proceedings of the Cambridge Philosophical Society*,Cambridge University Press, 53, (1957), 134–149 .

[11] M. Dehghan, J. Manafian, and A. Saadatmandi. Solving nonlinear fractional partial differential equations using the homotopy analysis method. *Numerical Methods for Partial Differential Equations: An International Journal*, 26(2) (2010), 448–479.

[12] J. S. Duan, R. Rach, D. Baleanu, and A. M. Wazwaz. A review of the Adomian decomposition method and its applications to fractional differential equations. *Communications in Fractional Calculus*, 3(2) (2012), 73–99.

[13] G. Espinosa-Paredes, M. A. Polo-Labarrios, E. G. Espinosa-Martínez, and E. del Valle-Gallegos. Fractional neutron point kinetics equations for nuclear reactor dynamics. *Annals of Nuclear Energy*, 38(2) (2011), 307–330.

[14] S. Ezz-Eldien, J. Machado, Y. Wang, and A. Aldraiweesh. An algorithm for the approximate solution of the fractional riccati differential equation. *International Journal of Nonlinear Sciences and Numerical Simulation*, 20(6) (2019), 661–674.

[15] A. F. Fareed, M. S. Semary, and H. N. Hassan. An approximate solution of fractional order riccati equations based on controlled picard's method with atangana–baleanu fractional derivative. *Alexandria Engineering Journal*, 61(5) (2022), 3673–3678.

[16] T. J. Freeborn. A survey of fractional-order circuit models for biology and biomedicine. *IEEE Journal on Emerging and Selected Topics in Circuits and Systems*, 3(3) (2013), 416–424.

[17] R. Gharechahi, M. Arabameri, and M. Bisheh-Niasar. Numerical solution of fractional bratus initial value problem using compact finite difference scheme. *Progr. Fract. Differ. Appl*, 7 (2021), 103–115.

[18] F. Ghomanjani and S. Shateyi. Numerical solution for fractional bratus initial value problem. *Open Physics*, 15(1) (2017), 1045–1048.

[19] S. Guo and L. Mei. The fractional variational iteration method using he's polynomials. *Physics Letters A*, 375(3) (2011), 309–313.

[20] I. Hashim, O. Abdulaziz, and S. Momani. Homotopy analysis method for fractional ivps. *Communications in Nonlinear Science and Numerical Simulation*, 14(3) (2009), 674–684.

[21] T. Jin and X. Yang. Monotonicity theorem for the uncertain fractional differential equation and application to uncertain financial market. *Mathematics and Computers in Simulation*, 190 (2021), 203–221.

[22] C. Li and F. Zeng. *Numerical methods for fractional calculus*, CRC Press, 24 (2015).

[23] R. Lyons, A. S. Vatsala, and R. A. Chiquet. Picards iterative method for caputo fractional differential equations with numerical results. *Mathematics*, 5(4) (2017), 65.

[24] Z. Odibat and S. Momani. Modified homotopy perturbation method: application to quadratic Riccati differential equation of fractional order. *Chaos, Solitons & Fractals*, 36(1) (2008), 167–174.

[25] Z. Odibat, S. Momani, and V. S. Erturk. Generalized differential transform method: application to differential equations of fractional order. *Applied Mathematics and Computation*, 197(2) (2008), 467–477.

[26] K. B. Oldham. Fractional differential equations in electrochemistry. *Advances in Engineering software*, 41(1) (2010), 9–12.

[27] S. Patnaik and F. Semperlotti. Application of variable-and distributed-order fractional operators to the dynamic analysis of nonlinear oscillators. *Nonlinear Dynamics*, 100(1) (2020), 561–580.

[28] I. Podlubny. *Fractional differential equations: an introduction to fractional derivatives, fractional differential equations, to methods of their solution and some of their applications.* Mathematics in science and engineering. Academic Press, London, (1999).

[29] A. Saadatmandi and M. Dehghan. A legendre collocation method for fractional integro-differential equations. *Journal of Vibration and Control*, 17(13) (2011), 2050–2058.

[30] M. S. Semary, H.N. Hassan, and A. G. Radwan. Single and dual solutions of fractional order differential equations based on controlled picard's method with simpson rule. *Journal of the Association of Arab Universities for Basic and Applied Sciences*, 24 (2017), 247–253.

[31] J. Shen, T. Tang, and L. L. Wang. *Spectral methods: algorithms, analysis and applications*, volume 41. Springer Science & Business Media, (2011).

[32] L. Song and W. Wang. A new improved Adomian decomposition method and its application to fractional differential equations. *Applied Mathematical Modelling*, 37(3) (2013), 1590–1598.

[33] M. Tafakkori-Bafghi, G. Barid Loghmani, M. Heydari, and X. Bai. Jacobi-picard iteration method for the numerical solution of nonlinear initial value problems. *Mathematical methods in the applied sciences*, 43(3) (2020), 1084–1111.

[34] M. Tafakkori-Bafghi, G. Loghmani, and M. Heydari. Numerical solution of two-point nonlinear boundary value problems via legendre–picard iteration method. *Mathematics and Computers in Simulation*, 199 (2022), 133–159.

[35] G. C. Wu and E. Lee. Fractional variational iteration method and its application. *Physics Letters A*, 374(25) (2010), 2506–2509.

Soheyla Ansari
Department of Mathematical Sciences
Ph.D. Student
Yazd University
Yazd, Iran
E-mail: sansari@stu.yazd.ac.ir

Mohammad Hossein Akrami
Department of Mathematical Sciences
Associate Professor of Mathematics
Yazd University
Yazd, Iran
E-mail: akrami@yazd.ac.ir